

First super-high-resolution model projection that the ancient “Fertile Crescent” will disappear in this century

Akio Kitoh¹, Akiyo Yatagai² and Pinhas Alpert³

¹Meteorological Research Institute, Tsukuba, Japan

²Research Institute for Humanity and Nature, Kyoto, Japan

³Tel Aviv University, Tel Aviv, Israel

Abstract:

The first full projections of rainfall and streamflow in the “Fertile Crescent” of Middle East are presented in this paper. Up until now, this has not been possible due to the lack of observed data and the lack of atmospheric models with sufficient resolution. An innovative super-high-resolution (20-km) global climate model is employed, which accurately reproduces the precipitation and the streamflow of the present-day Fertile Crescent. It is projected that, by the end of this century, the Fertile Crescent will lose its current shape and may disappear altogether. The annual discharge of the Euphrates River will decrease significantly (29–73%), as will the streamflow in the Jordan River. Thus countermeasures for water shortages will become much more difficult.

KEYWORDS Fertile Crescent; global warming; water resource; climate change; streamflow

INTRODUCTION

The Fertile Crescent is a region where ancient civilizations have developed. Population increases and intermittent dry spells in the region have resulted in agricultural innovations (Bellwood, 2004). This region runs northwards from the Jordan Valley, through inland Syria, into southeastern Turkey (Anatolia), eastwards through northern Iraq, and finally southeastward along the Zagros foothills of western Iran. Prevailing climatic conditions during ancient times allowed the first rain-fed agriculture in human history. Winter rainfall and snow in high mountains in the north were the main sources of water. At present, however, most of this region requires irrigation systems to sustain agricultural production. Recent satellite images show that some of the vegetation in the fertile Mesopotamian marshlands has disappeared (National Geographic News, 2001). Middle East contains a heavily utilized water basin and relies upon trans-boundary rivers to recharge artificial reservoirs. Several counteracting international projects are underway (UNEP, 2001) and the projections of future water availability are indispensable (Alpert, 2004, Alpert *et al.*, 2006, 2007).

It is widely accepted that the global and regional scale water cycle has been changing since the last century due to the accumulation of anthropogenic greenhouse gases and land use/land cover changes (IPCC, 2007). The increase in the world’s population (UNFPA, 2005) has brought increases in water usage for food production, flood damage due to urbanization, water pollution, drought, an overall increase in water

demand (Vörösmarty *et al.*, 2000). Water in the environment is an international problem because it is strongly related with the import and export of agricultural and industrial products and the economic and social well-being. Multi-model climate change simulations for the 21st century showed a decrease in runoff in the Middle East of up to 30% by 2050 (Milly *et al.*, 2005). A 40% decrease in the annual streamflow of the Euphrates River has also been projected (Nohara *et al.*, 2006). However, the horizontal resolution of the climate models used for these projections (between 400 km and 125 km) is not sufficient to resolve the topography in the Fertile Crescent. Thus far, only regional models have been able to resolve the necessary topography (Evans *et al.*, 2004). As the mountains are the source of the water that maintains the life and culture in this region, a high-resolution model that is able to accurately resolve topography is necessary to project future changes in water resources.

Recently, a global climate model with a horizontal grid size of about 20 km has been developed (Mizuta *et al.*, 2006). The increased horizontal resolution allows this model to realistically represent the topography of the area. This enables us to project the hydrological impact of climate change, particularly over those water-source regions, such as in Eastern Turkey, containing steep mountains. The horizontal resolution of this model is even higher than that of most regional climate models used worldwide, thus orographic rainfall is represented well in this model at the regional scale (Yatagai *et al.*, 2005). We are now entering a new era in which regional-scale climate information (down to a 20 km grid interval) is available without the use of regional models. The “time-slice” method was adopted to perform global warming simulations using this model.

MODEL AND EXPERIMENT

GCM

The atmospheric general circulation model (GCM) used in this study is a climate-model version of the Japan Meteorological Agency’s (JMA) operational numerical weather prediction model. The simulations were performed at a triangular truncation 959 with linear Gaussian grid (TL959) in the horizontal. The transform grid uses 1920 × 960 grid cells, corresponding to a grid size of about 20 km. The model has 60 layers in the vertical with the model top at 0.1 hPa. A detailed description of the model is given in Mizuta *et al.* (2006).

Mizuta *et al.* (2006) showed that modeled global distributions of the seasonal mean atmospheric circulation fields, surface air temperature and precipitation agree well with the observations. Moreover, the model improves the representation of regional-scale phenom-

Correspondence to: Akio Kitoh, Meteorological Research Institute, 1-1 Nagamine, Tsukuba, Ibaraki 305-0052, Japan. E-mail: kitoh@mri-jma.go.jp. ©2008, Japan Society of Hydrology and Water Resources.

Received 24 August 2007
Accepted 4 December 2007

ena and local climate, such as precipitation maxima to the west of the Western Ghats in southern India and along a southern periphery of the Himalaya range, by increasing horizontal resolution to better express topographical effects and physical processes without degrading the representation of global climate. Model topography of the target region in this study is shown in Figure 1a.

Experiment

We have performed three “time-slice” 10-year simulations. One (present run) is a present-day climate simulation using the observed climatological sea surface temperature (SST) (1982–1993, 12-year mean). The other two used the observed climatological SST plus SST differences between the present (1979–1998, 20 year mean of the 20C3M (20th Century Climate in Coupled Models project) simulation) and the future (2080–2099, 20 year mean). This difference in SST was obtained from climate change simulations based on the IPCC SRES A1B emission scenario. Approximate CO₂ atmospheric concentrations corresponding to the present and future cases are 348 ppm and 659 ppm, respectively. We used SST differences from two climate models with different climate sensitivity, i.e. with moderate climate sensitivity (MRI-CGCM2.3.2, Yukimoto *et al.*, 2006) and with high climate sensitivity (MIROC 3.2(hires), K-1 Developers, 2004). The changes in global annual mean SST are 1.6°C for the former and 3.2°C for the latter.

In the following, we denote the present run with the 20-km mesh AGCM as PC (present climate), the future run with moderate climate sensitivity as FM (future moderate), the future run with high climate sensitivity as FH (future high). The annual mean surface air temperature change in the targeted region (20°E–60°E, 20°N–50°N) is 2.6°C for FM–PC and 4.8°C for FH–PC.

River model

The river flow model used in this study is GRiveT (Global River flow model using TRIP) developed at MRI, where the TRIP (Total Runoff Integrating Pathways) is a global river channel network in a 0.5-degree grid (Oki and Sud, 1998). The effective flow velocity is set at 0.40 m/s for all rivers following studies that use flow velocities ranging from 0.3 to 0.5 m/s (Oki *et al.*, 1999). Note that it is known that flow velocities are not constant and can vary widely from 0.15 to 2.1 m/s (Arora and Boer, 1999). In the process of simulation, GRiveT distributes the runoff water on the model grids into TRIP grids with a weight that is estimated by the ratio of the overlaid area on both grids. GRiveT then transports the runoff water to the river outlet along the river channel through TRIP. GRiveT does not account for any human consumption or natural losses of the river water.

RESULTS

The simulated annual precipitation in the targeted region for the present-day (Figure 1c) compares well with the observed data (Figure 1b). We used the high-resolution climatological precipitation data set in East Mediterranean region derived by Yatagai (2006), which is based on the algorithm of Xie *et al.* (2007). The PC run clearly reproduces the orographic rainfall along the Mediterranean and the Black Sea coast, as well as over the Caucasus Mountains. A crescent-shaped large precipitation belt from Israel and the Adana region in Turkey through the region along the Zagros Mountains

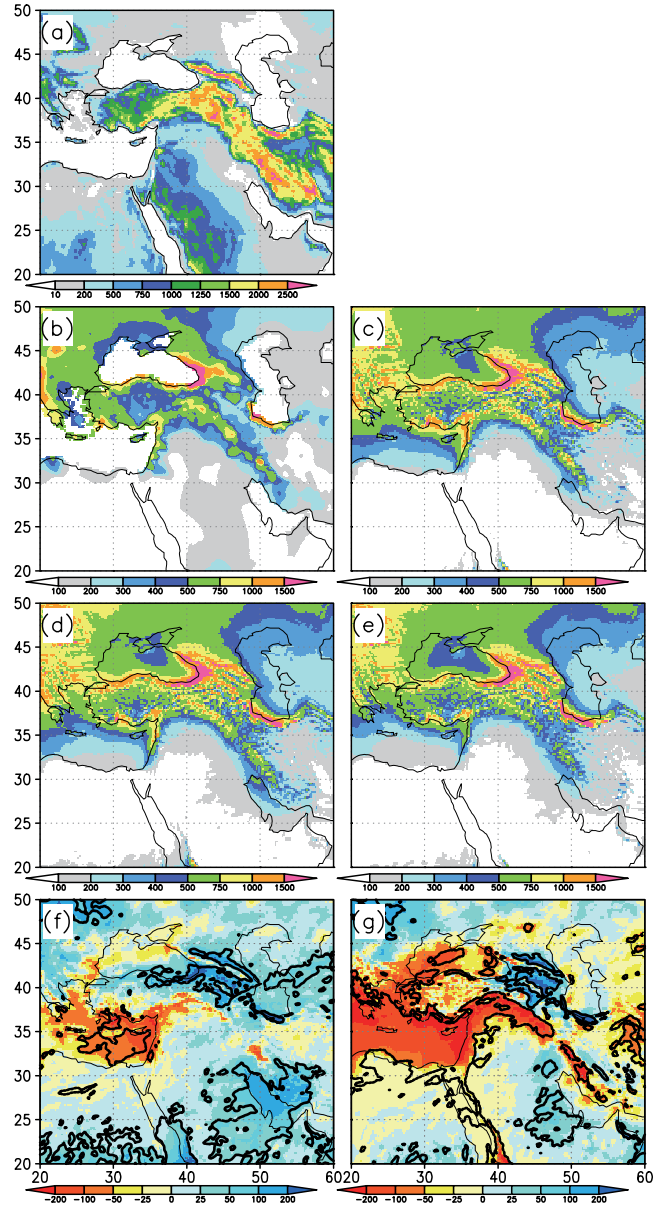


Figure 1. (a) Model topography in m. (b–g) Annual precipitation in mm. (b) East Mediterranean climatology. (c) AGCM present-day climatology (PC run). (d) Future (2081–2100) with the moderate-warming scenario (FM). (e) Future (2081–2100) with the high-warming scenario (FH). (f) Future (2081–2100) change in FM–PC. The contour indicates statistically significant at 90% level. (g) As in (f) but for FH–PC.

is also well reproduced. This is the first simulation of the “Fertile Crescent” shape of precipitation and the orographic precipitation to the south of the Caspian Sea in the history of AGCM. Although this observation data (Yatagai, 2006) uses more in situ gauge data over Iran and Turkey than the previously-published rainfall data sets, the density of the rain gauge stations is still not great enough over the mountainous regions, thus the “observed” rainfall in the mountains may be underestimated.

In the FM run (Figures 1d, f), the projected decrease in precipitation is concentrated in the Mediterranean Sea and coastal areas of Southern Turkey, Syria,

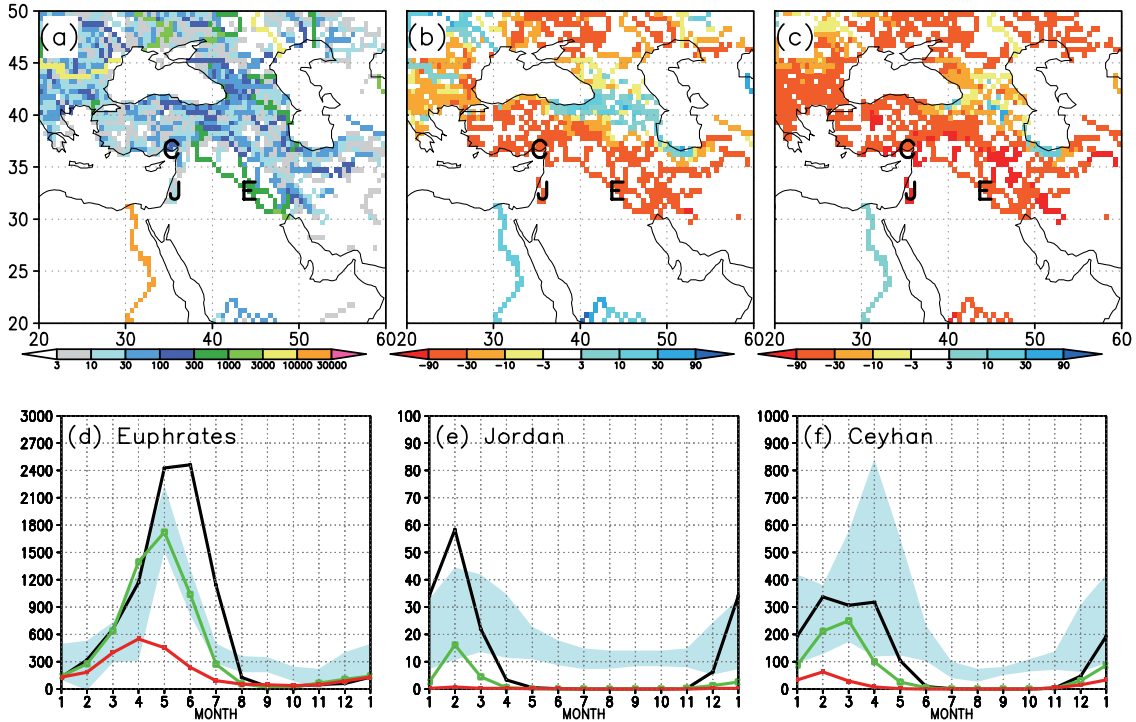


Figure 2. (a-c) Annual streamflow. (a) AGCM present-day climatology (PC run). Unit is $m^3 s^{-1}$. (b) Percentage change (%) in annual streamflow from the present-day simulation (PC) to the future (2081–2100) with the moderate-warming scenario (FM). (c) As in (b) but for the high-warming scenario (FH). (d-f) Monthly hydrographs for the Euphrates, Jordan and Ceyhan rivers. Black: AGCM present-day climatology (PC). Green: Future in FM. Red: Future in FH. Unit is $m^3 s^{-1}$. The shading denotes observed climatological mean plus/minus one standard deviation obtained from the Global River Discharge Center (GRDC; in Koblenz, Germany): Hindiya station in Iraq (44.27°E, 32.72°N) for the Euphrates River, and Misis station in Turkey (35.63°E, 36.97°N) for the Ceyhan River. The Jordan River record is obtained from Alon Rimmer (personal communication) and thanks to the Israeli Hydrological Service for collecting the data. E, J, and C indicate approximate locations of three rivers in Figures 2a–c.

Lebanon and Israel. This decrease in precipitation is mainly projected in the winter and spring. Annual precipitation is projected to increase in the future over the Caucasus Mountains and the Gulf coastal region. This increase in precipitation is projected mainly in fall, thus detailed investigation is needed to clarify regional differences between the projected precipitation changes. The FH run (Figures 1e, g) shows an anomaly pattern similar to the FM run, but even a larger precipitation decrease is projected over the Mediterranean Sea, Greece, the Black Sea, Turkey and the Fertile Crescent area. Precipitation increase over the Caucasus Mountains and Saudi Arabia is also projected as in FM.

At the end of the 21st century, evaporation generally increases both in FM and FH. Therefore, even in the areas where precipitation increases, an increase in evaporation may overcompensate for the increase in precipitation leading to decreased surface runoff. For this reason, trends in the streamflow are not always the same as that of the precipitation. Using the monthly runoff simulated by the PC, FM and FH experiments, streamflow is calculated at 0.5 deg by 0.5 deg grids. Figure 2 illustrates the simulated annual mean streamflow for the present (PC) and projected streamflow changes in the future. Future changes in streamflow are shown in percent change relative to the present. Figure 2b shows that, in FM, the streamflow decreases in most of rivers in the East Mediterranean region, and increases in the Nile River and the Caucasus Mountain region. Streamflow decreases further in FH (Figure 2c). Even the rivers with increased streamflow in FM, which are

mainly found in the mountainous regions, have decreased in streamflow in FH. The Nile River still shows positive anomalies in annual streamflow in FH, but its magnitude becomes smaller than in FM.

Figure 2d–f illustrates the monthly hydrographs and discharge changes for the three rivers in the region at the closest point to the observation: Euphrates (44.25°E, 32.75°N), Jordan (35.75°E, 32.75°N) and Ceyhan (35.25°E, 36.75°N). Figure 2 clearly illustrates that the annual streamflow is projected to decrease in the future in these three rivers. The annual discharge for the Euphrates River will decrease by 29% in FM and by 73% in FH. In both runs, the decrease is largest during the high-water season. Percentage decrease in river discharge is larger at the Ceyhan River region in Turkey, where the FM run projects 39% decrease and the FH run projects 88% decrease. Along this river, tremendous decreases in streamflow, accompanied with greater warming, demands a thorough countermeasure against agricultural and other uses of water in this region. The situation is much worse in Jordan. Although uncertainty in projections is large in such a small drainage area, the modest warming case of the FM run projects an 82% decrease. The high warming (and less precipitation) case (FH) projects that the streamflow will almost disappear throughout the year (98% decrease). Since the water of the Jordan River is already a matter for high tension and conflict for the bordering countries (Alpert, 2004), attentions are indispensable.

DISCUSSION

This study clearly shows that the super-high-resolution model simulates orographic rainfall very well. The 20-km mesh AGCM reproduces regional maxima of rainfall along the coastal regions of the East Mediterranean and the Black Sea and along the south coast of the Caspian Sea. Lower resolution models used in climate projection studies, such as in Intergovernmental Panel on Climate Change (IPCC) Fourth Assessment Report, show much smoother maximum of precipitation over the Caucasus Mountains (IPCC, 2007). Precipitation over the Fertile Crescent region is also well reproduced by the 20-km mesh AGCM with local maxima of orographic rainfall along the Zagros Mountains. Projected changes in precipitation also differ qualitatively between the 20-km mesh model and the lower resolution models. Both the FM run and the FH run show increased precipitation over the Caucasus Mountains and some parts of Gulf Coast states. These differences in precipitation resulted in streamflow changes in these regions.

The current climate model projects decreasing precipitation in the Fertile Crescent region. Changes in streamflow become more severe, which may result in substantial damage to rain-fed agriculture in the Mesopotamia area. Ancient rain-fed agriculture enabled the civilizations to thrive in the Fertile Crescent region, but this blessing is soon to disappear due to human-induced climate change. The fate of people in this politically vulnerable region depends on global management of the limited available water. Countermeasures have been planned for a long time, and global climate models that sufficiently represent the Fertile Crescent and project its future change can now be utilized for such purposes.

ACKNOWLEDGEMENTS

This work is done under the framework of the Kyosei Project and KAKUSHIN program funded by MEXT. The calculations were performed on the Earth Simulator. AK is also supported by the CREST project "Sustainable Water Policy Scenarios for River Basins with Rapidly Increasing Population" funded by JST, AK/AY/PA by "Impact of Climate Changes on Agricultural Production System in Arid Areas (ICCAP)", and AK/AY by the Global Environment Research Fund (B-062). PA thanks the support by the BMBF through the GLOWA-Jordan River Project.

REFERENCES

- Alpert P. 2004. The water crisis in the E. Mediterranean - and relation to global warming? In *Water in the Middle-East and N. Africa*, Zereini F, Jaeschka W (eds.); Springer: 55-61.
- Alpert P, Krichak SO, Dayan M, Shafir H. 2006. Climatic trends over the Eastern Mediterranean: past and future projections. *CLIVAR Exchanges* 11(2): 12-13.
- Alpert P, Krichak SO, Shafir H, Haim D, Osetinsky I. 2008. Climatic trends to extremes employing regional modeling and statistical interpretation over the E. Mediterranean. *Global and Planetary Change* 60: (in press).
- Arora VK, Boer GJ. 1999. A variable velocity flow routing algorithm for GCMs. *Journal of Geophysical Research* 104 (D24): 30965-30979.
- Bellwood PS. 2004. *The first Farmers: Origins of Agricultural Societies*. Blackwell Publishing, Oxford, United Kingdom; 380 pp.
- Evans JP, Smith RB, Oglesby RJ. 2004. Middle East climate simulation and dominant precipitation processes. *International Journal of Climatology* 24: 1671-1694.
- IPCC. 2007. *Climate Change 2007: The Physical Science Basis. Contribution of Working Group I to the Fourth Assessment Report of the Intergovernmental Panel on Climate Change*, Solomon S, Qin D, Manning M, Chen Z, Marquis M, Averyt KB, Tignor M, Miller HL (eds.); Cambridge University Press: Cambridge, United Kingdom and New York, USA; 996 pp.
- K-1 Developers. 2004. *K-1 coupled model (MIROC) description*. K-1 Technical Report 1, Hasumi H, Emori S (eds.); Center for Climate System research, University of Tokyo: Tokyo, Japan; 34 pp.
- Milly PCD, Dunne KA, Vecchia AV. 2005. Global pattern of trends in streamflow and water availability in a changing climate. *Nature* 438: 347-350.
- Mizuta R, Oouchi K, Yoshimura H, Noda A, Katayama K, Yukimoto S, Hosaka M, Kusunoki S, Kawai H, Nakagawa M. 2006. 20-km-mesh global climate simulations using JMA-GSM model -Mean climate states-. *Journal of the Meteorological Society of Japan* 84: 165-185.
- National Geographic News. 2001. Ancient Fertile Crescent almost gone, satellite images show. http://news.nationalgeographic.com/news/2001/05/0518_crescent.html. Accessed: 24 August 2007.
- Nohara D, Kitoh A, Hosaka M, Oki T. 2006. Impact of climate change on river discharge projected by multi-model ensemble. *Journal of Hydrometeorology* 7: 1076-1089.
- Oki T, Nishimura T, Dirmeyer P. 1999. Assessment of annual runoff from land surface models using Total Runoff Integrating Pathways (TRIP). *Journal of the Meteorological Society of Japan* 77: 235-255.
- Oki T, Sud YC. 1998. Design of Total Runoff Integrating Pathways (TRIP) - A global river channel network. *Earth Interactions* 2: 1-37.
- UNEP. 2001. *The Mesopotamian Marshlands: Demise of an Ecosystem*. Technical Report UNEP/DEWA/TR.01-3, UNEP DEWA/GRID-Geneva: Switzerland; 58 pp.
- UNFPA. 2005. *State of World Population 2005*. UNFPA: New York, USA; 128 pp.
- Vörösmarty CJ, Green P, Salisbury J, Lammers RB. 2000. Global water resources: Vulnerability from climate change and population growth. *Science* 289: 284-288.
- Xie P, Yatagai A, Chen M, Hayasaka T, Fukushima Y, Liu C, Song Y. 2007. A gauge-based analysis of daily precipitation over East Asia. *Journal of Hydrometeorology* 8: 607-626.
- Yatagai A. 2006. An analysis of observed precipitation over the Fertile Crescent. The Advanced Report of ICCAP, RIHN: 17-20.
- Yatagai A, Xie P, Kitoh A. 2005. Utilization of a new gauge-based daily precipitation dataset over monsoon Asia for validation of the daily precipitation climatology simulated by the MRI/JMA 20-km-mesh AGCM. *Scientific Online Letters on the Atmosphere* 1: 193-196.
- Yukimoto S, Noda A, Kitoh A, Hosaka M, Yoshimura H, Uchiyama T, Shibata K, Arakawa O, Kusunoki S. 2006. Present-day climate and climate sensitivity in the Meteorological Research Institute GCM Version 2.3 (MRI-CGCM2.3). *Journal of the Meteorological Society of Japan* 84: 333-363.